



High resolution remote sensing observations for missions to the Jovian system: Io as a case study

Gregory T. Delory^{a,b,*}, Conor Laver^c, Imke de Pater^c, Joe Pitman^d, Alan Duncan^e

^a Space Sciences Laboratory, University of California, Berkeley, CA 94720, USA

^b NASA Ames Research Center, Moffett Field, CA 94035, USA

^c Department of Astronomy, 601 Campbell Hall, University of California, Berkeley, CA 94720, USA

^d Exploration Sciences, P.O. Box 24, Pine, CO 80470, USA

^e Lockheed Martin Advanced Technology Center, 3251 Hanover Street, Palo Alto, CA 94304, USA

ARTICLE INFO

Article history:

Received 9 February 2010

Received in revised form

7 July 2010

Accepted 2 August 2010

Available online 6 August 2010

Keywords:

Io

Remote sensing

Instruments

ABSTRACT

We present modeled images of Io at a variety of distances from the surface as a function of imager aperture size and wavelength. We consider the science objectives that could be achieved from missions engaged in long range remote-sensing of Io during the approach to the Jovian system and subsequently from orbit around Europa or Ganymede, in both the visible and near infrared wavelength ranges. We find that basic global mapping objectives in the visible can be met with a traditional 0.5 m telescope design. A more ambitious 1.5 m telescope could accomplish much more detailed objectives such as topographical measurements, and determination of flow patterns and thermal sources for individual active regions on Io.

© 2010 Elsevier Ltd. All rights reserved.

1. Introduction

Despite a multitude of spacecraft flybys (including *Voyager*, *Cassini*, and *New Horizons*), one spacecraft orbiter (*Galileo*, orbiting Jupiter), and ground-based monitoring for almost 30 years, there are still many unsolved questions regarding Io. Early *Voyager* maps showed this satellite to have a complex surface, mostly as a result of ongoing and vigorous volcanism (McEwen, 1988). With the *Galileo* mission, the technological progress of 15 years allowed more sensitive instruments to study Io. Close flybys allowed brief glimpses at fine spatial resolutions of tens to hundreds of meters. The SSI imager, NIMS infrared spectrometer, and other instruments have relayed a body of data back to Earth that is still being analyzed, providing a wealth of information to geologists and astronomers alike in their quest to understand Io's ephemeral appearance. Studies of the volcanic paterae and lava flows provided evidence of a young and fast changing surface (i.e., Geissler et al., 2004; Turtle et al., 2004; Douté et al., 2004). During the *Voyager* encounters, volcanic activity was mostly attributed to being driven by sulfur, because hot spot temperatures were measured to be less than ~600 K. High spatial resolution observations at infrared wavelengths, as enabled during close

Galileo encounters, and from the ground using adaptive optics (AO) techniques, showed that many of the volcanic eruptions were in fact at temperatures over 1000 K, similar to silicate volcanism on Earth (Johnson et al., 1988; Blaney et al., 1995; Marchis et al., 2002; Milazzo et al., 2005). On occasion even hotter eruptions were measured, exceeding those seen in Earth's current geologic era, suggestive of ultramafic lava compositions (McEwen et al., 1997, 1998; Williams et al., 2000). Apparently, spatial resolution is an important capability required to reveal the highest temperatures of erupting magmas, since the areal extent of the source vent, i.e., the source of the eruption, is usually very small. As the magma protrudes from the source vent, this small region will display the highest temperature, while the lava flows away from the source vent, it cools. Hence, the lava near an eruption site displays a continuous and large range of temperatures: a very small area of extreme high temperature (the vent), and increasingly larger areas at lower temperature, contributed by increasingly older lava flows. Low-resolution imagers detect thermal anomalies averaged over much of the eruption site, which makes it impossible to distinguish the small contribution of magma at the highest temperature, as the areal coverage of lava at lower temperatures overwhelms the thermal emission. Only through imagers at high spatial resolution can this component of the emission be detected.

During close passes, *Galileo*'s instruments performed detailed spectroscopic investigations of the local surface ices (composition, grain size, thickness) and terrain near volcanic centers (Douté et al., 2004), a vital step to understand the ongoing processes on Io. More recently the *New Horizons* mission passed by the Jovian

* Corresponding author at: Space Sciences Laboratory, University of California, Berkeley, CA 94720, USA. Tel.: +1 510 643 1991; fax: +1 510 643 8302.

E-mail address: gdelory@ssl.berkeley.edu (G.T. Delory).

Table 1
Model Io images.

Label	Wavelength	Distance	Pixel size	Observable features
3a	Visible	250,000 km	51 m	Crater walls, flow patterns
3b	Near IR	250,000 km	153 m	Discrete thermal sources within one caldera
3c	Visible	650,000 km	132 m	Crater walls, flow patterns
3d	Near IR	650,000 km	397 m	Crater sizes, Lava Lake overturn
3e	Visible	1,500,000 km	305 m	Crater sizes, Lava Lake overturn
3f	Near IR	1,500,000 km	915 m	Thermal measurements of local hotspots
4a	Visible	4 AU	122 km	Outburst detection
4b	Near IR	4 AU	365 km	Outburst thermal measurements, surface thermal flux
4c	Visible	2 AU	61 km	Multiple hotspot detection
4d	Near IR	2 AU	183 km	Global thermal variations, atmospheric density changes
4e	Visible	0.2 AU	6.1 km	Surface mapping, albedo variations
4f	Near IR	0.2 AU	18.3 km	Local thermal changes, accurate hotspot positions

system, capturing stunning images of an erupting plume at Tvashtar on Io (Spencer et al., 2007). It also provided new insight into UV auroral activity from observations taken when Io was in eclipse, i.e., in Jupiter's shadow (Retherford et al., 2007). Eclipse and, in particular, night-side observations are easiest to conduct by instruments in space, whether in nearby orbit or from distant vantage points. During such times, in the absence of the glare of reflected sunlight, very faint glows can be discerned. Similar measurements are possible from Earth when Io enters into Jupiter's shadow (Macintosh et al., 2003; de Pater et al., 2004, 2007); however, opportunities to observe such events with AO are rare, relatively short and challenging. Moreover, during these periods Io will always display the same hemisphere to Earth, while spacecraft observations can view any longitude on the satellite.

Numerous open questions and unsolved puzzles still exist, despite the multitude of observations from space and Earth (Williams et al., 2009). For example, the compositional range of magma is unknown, as is the composition of volcanic plumes. It is still not clear whether Io's atmosphere is dominated by volcanic gases or sublimation of surface frost.

The composition of magma is tied to the question of sulfur versus silicate volcanism: what is the contribution of sulfur volcanism to Io's heat flow, and how often and where are eruptions over 1600 K seen? Although Io's volcanic activity is clearly caused by the strong tidal heating that is induced by the orbital eccentricity forced by Jupiter and the 4:2:1 Laplace resonance between Io, Europa, and Ganymede, many details of this process are still unknown. We do not know, for example, where and how the heat is dissipated, nor do we know whether Io's heat flow is steady or episodic. These are just a few of many outstanding questions regarding Io, and several of these puzzles can be solved through regular and persistent observations at high spatial and moderate (\sim nm) spectral resolution. For example, high spatial and hyperspectral resolution data are needed to identify minerals on Io's surface. The composition and temperature of gas plumes and Io's atmosphere are best addressed through observations at high spectral resolution.

With future missions to the Jovian system currently in the planning stages, we present results of simulations using both Earth-analog and Io image models, showing how Io would likely appear to capable remote sensing payloads, both during approach and from a variety of long-range Jovian science orbits that assume either Ganymede or Europa as the principal targets. These images provide the framework for a discussion of the type of features one could hope to study and the trade-offs that should be considered when formulating requirements, concepts, and straw-man payload designs for such future missions. We note that although we use Io as an example for such observations, the idea

is generic: persistent, high resolution data are essential to solve many open questions in planetary science, ranging from planetary atmospheres (i.e., dynamics as in vortices, eddies, storm systems, and zonal flows), to satellite surfaces and planetary rings. Our study shows that high spatial resolution is feasible on many targets other than the immediate primary objective of a mission, and enables a host of Jovian system science objectives. In Sections 2 and 3, we discuss our models, and in Section 4 we give a summary of instrument concepts that could be used to provide the desired spatial and frequency resolution.

2. Model simulations

The model images (Table 1) presented here are derived from two sources. The high resolution images showing a single volcano from near and within the Jovian system (Fig. 3) are based on a satellite image of Mount St. Helens,¹ (Fig. 1), which had a size scale of 16.4 m/pixel. This image was chosen for illustrative purposes only, since it has a higher resolution than any existing image of Io itself, and shows a variety of volcanic features. The lower resolution images showing Io from the perspective of a spacecraft on approach to the Jovian system (Fig. 4) were based on the global high resolution Galileo/Voyager mosaic of Io (Fig. 2) produced by the US Geological Survey (Archinal et al., 2001).

Both models have been convolved and rebinned to match the pixel size and diffraction limit of representative 0.5 and 1.5 m telescopes used to bound the payload design space we considered. In all cases it has been assumed that the pixel size and position of the detector is designed to well sample (at two pixels per resolution element) the diffraction limit of the telescope, at the given wavelength. The diffraction limit scales as

$$\text{Diff. limit} = \frac{1.22 \times \text{Wavelength}}{\text{Telescope diameter}}$$

As a result, the effect on the image of increasing the telescope size by a factor of 3 (from 0.5 to 1.5 m) is equivalent to a decrease in the wavelength from the near IR (1500 nm) to the visible (500 nm). Thus we present two sets of images, the first being Io as seen in visible light by a 1.5 m telescope and the second can be considered as Io seen by a 0.5 m telescope in the visible or by a 1.5 m telescope in the infrared. While the spatial resolutions of the latter two examples are the same, the phenomena studied at these two wavelengths will differ. At visible wavelengths topographic features as mountains, calderas, volcanoes, and lava flows can readily be discerned, while images at near-infrared

¹ maps.google.com.



Fig. 1. A satellite image of Mt. St. Helens, taken from Google Maps at 16.4 m/px resolution.

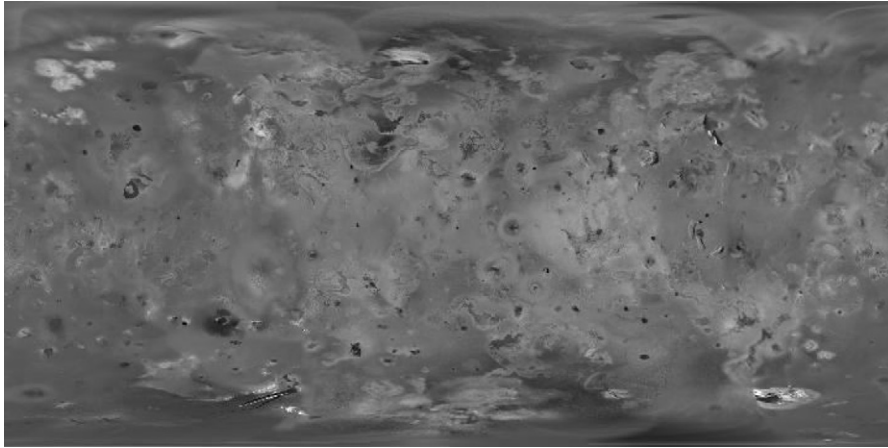


Fig. 2. Visible map of Io's surface from the high resolution Galileo Voyager mosaic (the longitude is shifted by $\sim 180^\circ$).

wavelengths reveal spatial variations in the satellite's (IR) albedo. The latter observations are also sensitive to volcanic hot spots, as the blackbody curves of hot spots usually peak at infrared wavelengths.

For the global images shown in Fig. 4, we used the global map of Io at a resolution of $\sim 0.5^\circ/\text{pixel}$, and re-projected this image back onto a sphere, taking into account the effect of the phase angle and the reflection from a spherical body. We approximate these effects using a Minnaert function (Minnaert, 1941), which has the advantage of being much simpler to apply than most models, with only two free parameters dependent on the surface material and roughness. It has the following form:

$$\left(\frac{I}{F}\right)_{\text{obs}} = B_0 \mu_0^k \mu^{k-1},$$

where I/F is the observed reflectance and μ_0 and μ are the cosines of the illumination and emission angles, respectively. B_0 and k are the Minnaert parameters and vary with composition and surface roughness. B_0 is similar to the normal albedo of the surface, while k is the limb darkening coefficient. Both parameters vary with wavelength and composition across Io's surface. Laver and de

Pater (2008) found that a globally averaged value of $k=0.75$, under the assumption that B_0 varies directly with albedo, gave the best limb correction for their K band ($2 \mu\text{m}$) images.

The distances we chose to model are representative for spacecraft bound for Europa and Ganymede. It is possible that future missions could be sent to pass much closer to Io or even orbit it; however, its location within the radiation belt of Jupiter would mean the spacecraft and its instruments would require significantly more radiation shielding, a much shorter mission lifespan and/or a reduced observing time.

3. Discussion

It is apparent from the images that the choice of telescope size and the observing distance will dramatically affect the science return. With a 1.5 m telescope, in the closest approach of a Europa orbiter (Fig. 3a), one can distinguish the individual shadows of terrain features from actual albedo variations on Io. This would enable the stereographic measurement of the altitude of such features. The fine-scale structure of the crater walls is apparent

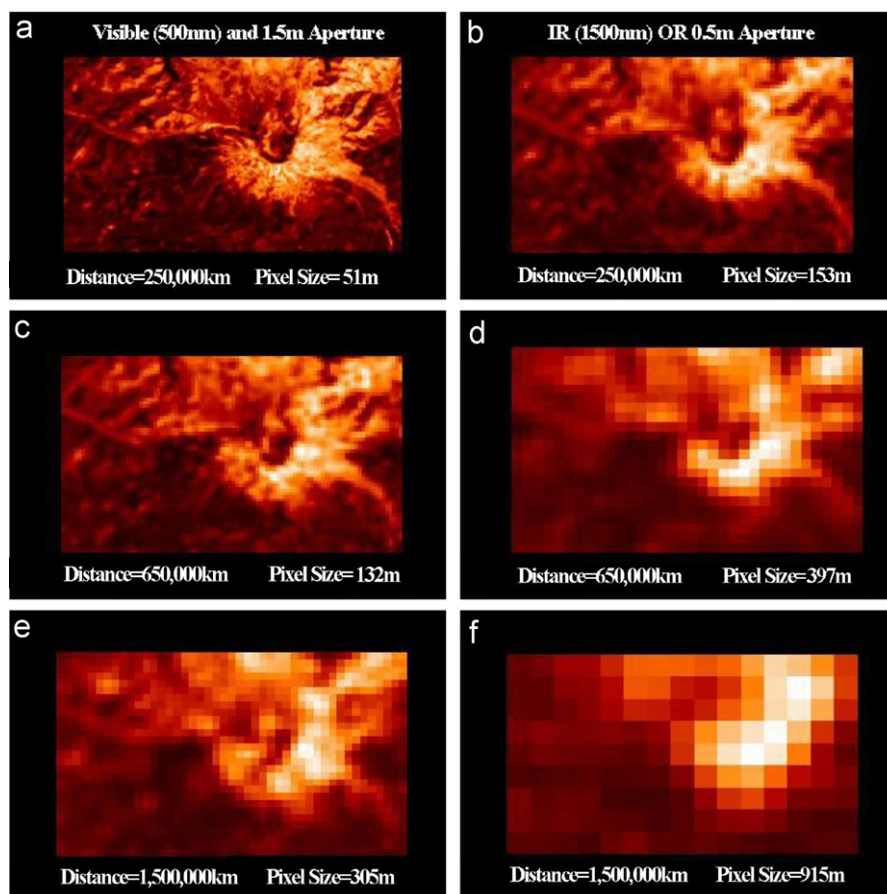


Fig. 3. Model images of Io for distances of 250,000 km (top), 650,000 km (middle), and 1.5 million km (bottom). The left column shows the models for a 1.5 m telescope observing at 500 nm (visible), while the right column can represent either a 0.5 m telescope observing in the visible or a 1.5 m telescope observing at 1500 nm in the near infrared. The original image is the satellite image of Mt. St. Helens shown in Fig. 1.

and the surrounding flows could be measured. Such measurements are made much more difficult with a smaller telescope in the visible (0.5 m) or the larger 1.5 m telescope operated at infrared wavelengths, as seen in Fig. 3b. With the lower resolution it is still possible to measure features such as crater size, or the extent of lava lakes such as seen at Pele and Loki. In the case of the latter it would be highly desirable to accurately pinpoint the location of thermal emissions to test models of Loki's recurrent activity. It has been proposed that volcanic eruptions at Loki, seen at near-infrared wavelengths, may be explained by a periodic overturn of the lava lake (Rathbun et al., 2002). Observations at the resolutions such as those seen in Fig. 3b and c should be able to confirm this model, and monitor and measure the rate of such overturn.

Moving to lower resolutions such as at the closest approach of a Ganymede orbiter for an infrared/smaller telescope (Fig. 3d) or Io–Ganymede at their furthest separation observed in the visible with the larger aperture of 1.5 m (Fig. 3e), it becomes substantially more difficult to distinguish shadows from true albedo changes. Without a detailed topographic map, modeling the extent and effect of shadows of large geographical features from a single image is impossible, and observations at a variety of phase angles would be required to determine the true albedo of the surface features. All fine details of the surrounding terrain also become significantly blurred; the main measurements possible would be estimates of crater size and the measurement of large scale lava flows and emplacements. With Ganymede and Io at the furthest separation and when observations are taken with the 0.5 m telescope or in the infrared with the 1.5 m

telescope (Fig. 3f), we approach the limit of being able to study the local environment of individual hotspots and move towards global measurements of albedo variations and thermal flux. It should be noted that some measurements at sub-optimal distances will be required, as both Io and the moons around which these orbiters will be positioned are tidally locked with Jupiter, such that the same face of Io is being observed at each closest approach. To achieve full longitudinal coverage of Io's surface, a range of observations at various distances will be required.

It is also interesting to examine what such telescopes could do before the spacecraft arrives at a given science orbit (Fig. 4). Space-based instruments have an obvious advantage over terrestrial telescopes; assuming they can be held sufficiently stable to avoid jitter, there is no blurring or extinction by the Earth's atmosphere (i.e., the entire wavelength range can be observed). However, given the size and mass budgets of such missions, unlike their terrestrial counterparts these instruments might have smaller diameter apertures and lower intrinsic spatial resolution. As can be seen in Fig. 4c, once the mission reaches about halfway to its destination, near 2 AU from Io, the images begin to approach those that can be obtained by modern terrestrial instruments. In fact if we assume a diameter of 1.5 m, then the instrument will show an improvement over the AO instruments on large terrestrial telescopes, such as at the 10 m W.M. Keck observatory, 8 m European Southern Observatory (ESO) and Gemini Telescopes, during the final seventh of its flight (about 0.6 AU, or 1200 Jupiter radii, from Io). The highest resolution image shown in Fig. 4e and f shows the best images possible at

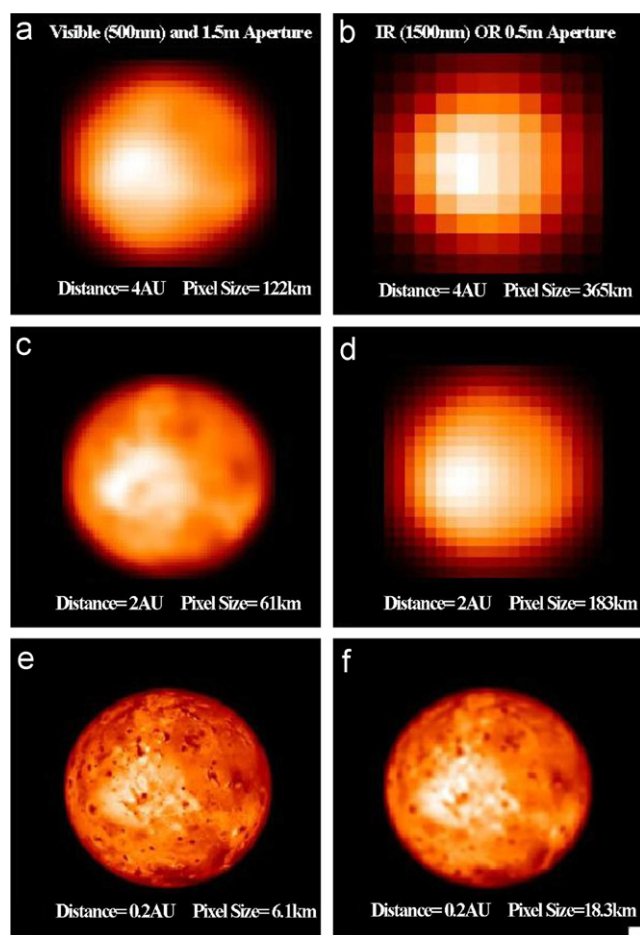


Fig. 4. Model images of Io for distances of 4 AU (top), 2 AU (middle), and 0.2 AU (bottom). The left column shows the models for a 1.5 m telescope observing at 500 nm (visible), while the right column can represent either a 0.5 m telescope observing in the visible or a 1.5 m telescope observing at 1500 nm in the near infrared.

0.2 AU, or 420 Jupiter radii. These images are also equivalent to those that would be taken by the proposed next generation Thirty Meter Telescope (TMT), assuming perfect AO correction.

In general, the science goals that could be achieved during the approach phase are a more refined version of what is currently being done from the ground or Earth orbit such as global mapping of hot spots (Marchis et al., 2003), spectral analytic maps of the surface composition that can be used to search for features such as new deposits around volcanic eruptions (i.e., the red rings surrounding Pele and Tvashtar), temporal changes in the abundance and grain size of sulfur dioxide frost on the surface (Douté et al., 2001, 2004; Laver and de Pater, 2008), and determining the spatial distribution of atmospheric density and composition (e.g., McGrath et al., 2000; Spencer et al., 2005). Observations of Io entering and leaving Jupiter's shadow can be scheduled much easier without the constraints of Earth's diurnal spin and the requirements of AO observations. Eclipse observations will reveal the faintest hot spots, as well as auroral and plume emissions; using spectroscopy, the gases which produce the emissions can be identified, such as gaseous sulfur monoxide (de Pater et al., 2002, 2007).

4. Instruments and missions

Future missions to the Jovian system could provide numerous opportunities for both distant viewing and detailed mapping of Io.

For missions focused on targets other than Io, opportunistic remote observations could take place provided that the spacecraft carries visible or infrared cameras and spectrometers with sufficient resolving capability. As yet undefined New Frontiers class missions could enable remote imaging of Io at a variety of distances and resolutions depending on the orbit details. Future flagship class missions include the US built Europa orbiter and a European built Ganymede Orbiter, which together will study the Jovian system in depth. Both the Europa and Ganymede orbiters would enable regular monitoring of Io. An orbiter about Europa would pass its point of closest approach to Io once every 4 days at a distance of approximately 250,000 km (Fig. 3a and b), while a Ganymede orbiter would reach a closest approach of 650,000 km once every 2.5 days (Fig. 3c and d). These remote observations could potentially provide detailed characterization and monitoring of Io's surface while these missions obtain their primary measurements around their respective target moons.

In both planetary and terrestrial remote sensing applications, there has been a continual trend toward the acquisition of higher resolution imagery in order to discern the temporal and spatial scales of interest. This trend is evident in the Mars Exploration Program, culminating in the development of the 0.5 m aperture high resolution imaging science experiment (HiRISE) now flying on the Mars Reconnaissance Orbiter (MRO), which regularly yields sub-meter resolution imagery (McEwen et al., 2010). The IKONOS satellite camera is another example of a large, 70 cm aperture imager that similarly helped reveal sub-meter resolution imagery of Earth for scientific and commercial purposes. Looking toward the future, we considered in our simulations that aperture sizes approaching the upper bound may be enabled by the use of distributed aperture technology, which is much smaller in overall payload volume than conventional monolithic telescope designs having the same resolution. Here we discuss the utility of these approaches, focusing on imaging cameras with varying spectral capabilities, using the solid state imaging (SSI) camera on the Galileo mission as a performance benchmark (Table 2). The SSI camera (Fig. 5) design utilized a Cassegrain telescope with a ~ 17.6 cm aperture, and covered a wavelength range of 0.375–1.1 μm that could be sub-divided using 7 filters (Belton et al., 1992). Along with the other imagers and spectrometers on Galileo, SSI required accommodation on a scan platform. The highest resolution images obtained by the SSI were due in large part to the series of close fly-bys of the largest moons achieved by the Galileo spacecraft. Europa was mapped at ~ 10 m resolution over $\sim 1\%$ of its surface, and at 100 m resolution over 10% of the surface. A series of flybys over Io at closest approach ranges of hundreds to thousands of km yielded images between 5 and 500 m/pixel (McEwen et al., 2000), and enabled the characterization of lava lakes, flows, calderas, and many other features that we considered in our simulated study (Table 1). The SSI data obtained during these fly-bys has indeed been instructive in terms of the potential for high resolution imagery to yield a significant science return. A prime motivation to conduct the simulations we have presented was to understand what current and future instruments could provide similar potential science return from remote observations at 250,000 km or more, without requiring fly-bys of all targets of interest.

Though its operations have encountered some detector performance difficulties (Bergstrom et al., 2004), effective work-arounds have allowed HiRISE (Fig. 6) to provide global samples of stunning new imagery of many important surface details on Mars (McEwen et al., 2010). The HiRISE telescope has clearly established a 0.5 m aperture, near-diffraction limited capability for orbiters on planetary science missions. Because of its conventional design, it possesses a nearly 1.6 m long telescope that proves challenging for spacecraft packaging, as well as a fixed

Table 2
Comparison of past, current, and future imaging systems for planetary science missions.

System	Aperture size	System resources	Spectral capability	Ground sample distance (GSD)	
				100 km	250,000 km
Galileo SSI	17 cm	29 kg, 90 cm × 25 cm × 30 cm, 23 W	8 filters, 375–1100 nm	~1 m/px	~2.5 km/px
HiRISE	0.5 m	65 kg, 113 cm × 59 cm dia, 125 W	3 band multispectral, 400–1000 nm	~0.10 m/px	~250 m/px
IKONOS	0.7 m	171 kg, 1.52 m × 0.79 m dia, 350 W	4 band multispectral, 445–853 nm	~0.12 m/px	~200 m/px
MIDAS	1.5 m	250 kg, 1.6 m × 1.6 m × 1.5 m, 200 W	Imaging spectrometer ~nm resolution	~2 cm/px	~50 m/px

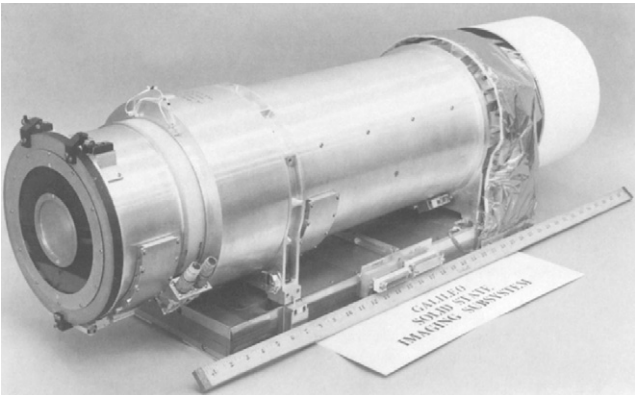


Fig. 5. The Galileo SSI (Belton et al., 1992), derived from Voyager-era heritage, was able to achieve high resolution imagery of the largest Jovian moons during a series of close fly-bys.



Fig. 6. High Resolution Imaging Science Experiment (HiRISE) Credit NASA/JPL/UofA <<http://marsoweb.nas.nasa.gov/HiRISE/instrument.html>>.

body-pointed implementation that hence dominates spacecraft operations once in-orbit.

In terrestrial applications, larger aperture sizes have been in use since the mid 1990s, when commercial industry brought forth a 70 cm diffraction-limited optical imager for Earth observations from low earth orbit (LEO) aboard the IKONOS satellite (Ryan et al., 2003; Dial et al., 2003). Originally intended as a pair of free-flying imagers, launch vehicle failure of the first mission resulted in having only one operational IKONOS, starting in 1999. As the first in a series of commercially accessible space-based imaging resources providing sub-meter resolution imagery, for over 7 years of operations the IKONOS camera images have helped advance many fields of Earth science, from land change to coastal mapping in stereo, as well as many civilian needs, such as rapid response images in areas struck by tsunamis and earthquakes. The IKONOS camera uses a 70 cm polished and lightweight glass primary mirror coupled to both panchromatic and multispectral

sensors, carried on an agile spacecraft bus capable of rapidly repointing and stabilization. It operated in a nominal 681 km altitude sun-synchronized orbit, providing as good as 82 cm ground sample distance (GSD) panchromatic resolution when pointed Nadir as well as lower resolution (~4 m) imagery in four multispectral bands. As in the case of HiRISE, IKONOS is a testimony to the utility of larger aperture spaceborne systems for Earth and planetary science.

While both HiRISE and IKONOS have achieved a significant science return, the accommodation of traditional monolithic telescope designs quickly reaches both volume and mass limits given the proportional growth in focal lengths required for conventional three-mirror anastigmat (TMA) optical design approaches. The upper bound aperture size of 1.5 m we considered in our study, roughly ~60% of the diameter of the Hubble Space Telescope primary mirror, may prove too difficult to implement on near term planetary orbital platforms. However, such large aperture sizes may be obtained synthetically, without the proportional growth in telescope length, using distributed aperture technology (Lucke, 2001). The multiple instrument distributed aperture sensor (MIDAS) is one example of such a system (Stubbs et al., 2004), combining individual smaller telescopes in an array configuration that yields resolved images the equivalent of a single aperture of the overall array size (Fig. 7). A 1.5 m aperture size version of MIDAS was studied under the NASA high capability instruments for planetary exploration program in preparation for the Jupiter Icy Moons Orbiter (JIMO) and other outer planet missions (Pitman et al., 2004a, b). The MIDAS design is inherently compact; its overall length, including a scan platform, is approximately equal to its overall diameter, and is thus less likely to encounter volumetric constraints on an orbiter. MIDAS operates independently as nine redundant smaller collector telescopes, or phased as a wide-field imaging array having the diffraction limit of a monolith equivalent to the overall array diameter. A distributed aperture system can also accommodate a number of “back-end” specialized imagers or spectrometers, optimized for specific tasks. In this example, MIDAS accommodates a suite of up to six modular back-end science instruments, such as for complementary cameras and spectrometers, each accessing the telescope focal plane. MIDAS also enables the capability to retrieve spectral information, since the delay lines used to phase the MIDAS image plane can also be employed as a Fourier Transform Imaging Spectrometer (IFTS) (Kendrick et al., 2003, 2006). In our studies to date, a 1.5 m aperture MIDAS payload on a Jovian mission was found to require physical resources of about 250 kg, and roughly 200 W of power. While substantial, this estimate includes six back-end spectrometers and imagers as well as a scan platform, and thus could be within the realm of flagship class missions assuming a high degree of sensor integration. For example, the remote sensing suite on the Cassini mission, consisting of all spectrometers and cameras, required approximately 183 kg of mass and 155 W of power to implement. Whereas, a 1.5 m MIDAS design requires approximately 50% more mass and power resources, it could provide the same spectral coverage at increased resolution,

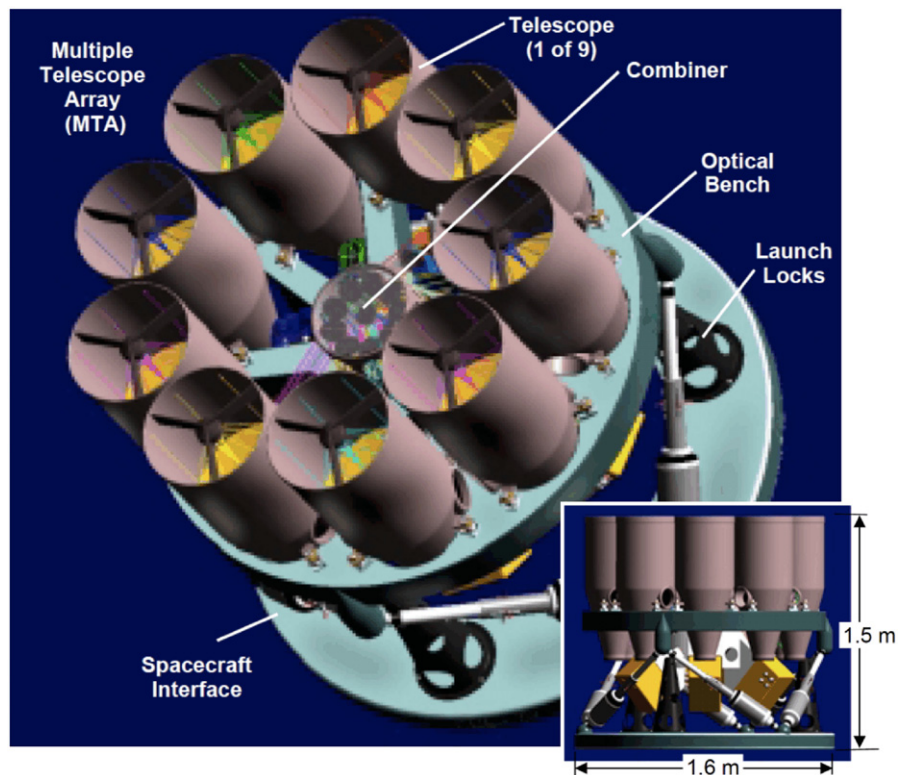


Fig. 7. The MIDAS assembly enables imaging spectroscopy at large aperture sizes without a corresponding increase in telescope length, resulting in a modular form factor smaller than traditional monolithic telescope designs.

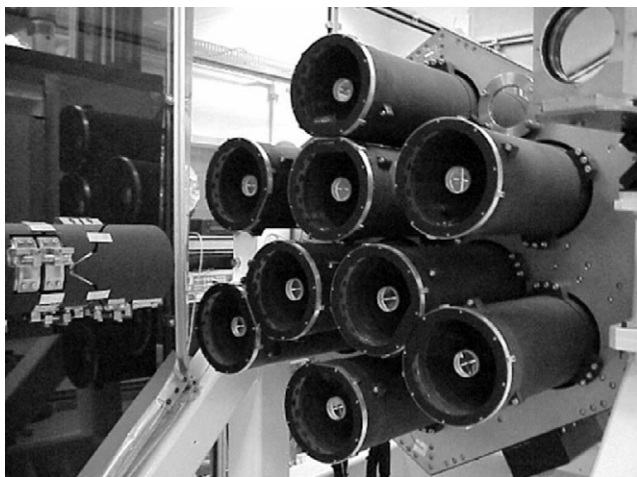


Fig. 8. The STAR9 testbed uses nine telescopes in an array similar to the MIDAS concept proposed for outer planet missions (Kendrick et al., 2006).

and includes a scan platform to facilitate flexible operations. Moreover, the MIDAS approach is to a certain degree scalable. Prior scaling studies showed that resource allocations of about 1 m³, 200 kg, and 150 W could support a 1.0 m aperture version. This would then represent resources comparable to the Cassini remote sensing payload, while enabling substantially higher resolution. Unlike the other example instruments covered here, distributed aperture imaging has yet to establish a heritage in planetary science mission applications. However, this technology has been in development for well over 2 decades (Zarifis et al., 1999) and considerably advanced for use on other applications of

national interest (Kendrick et al., 2006). Furthermore, several generations of full-scale high-fidelity laboratory testbeds of distributed aperture systems have been developed such as Star-9 (Kendrick et al., 2006) (Fig. 8), as well as a design study for MIDAS (Smith et al., 2005).

Fig. 9 shows the relative resolution obtained as a function of various aperture sizes over the ranges considered in our study, including a Galileo SSI-class system for reference. Aperture sizes of 0.5 m or more can effectively image many of the detailed features of interest on Io (< 1 km/px, Table 1 and Fig. 3) from 250,000 km, i.e., from the vantage point of Europa. In contrast, a Galileo SSI-class camera would be required to pass within 100,000 km or closer to achieve this resolution. The 0.5 m aperture size can effectively perform global mapping of Io from either Europa or Ganymede. Both 0.5 and 1.5 m systems could perform local mapping of the terrain near volcanic centers on Io from the position of Europa (Fig. 3a and b); from Ganymede, this is possible only with a 1.5 m aperture. The 1.5 m aperture system on a future Jovian mission would enable visible imaging of Io at the resolutions on the left side of Fig. 3 (a, c, e), simultaneously with infrared images obtained at the resolutions on the right (Fig. 3b, d, f), over distances that include observations from Europa, Ganymede, and the approach phase.

5. Conclusion

Io remains one of the most enigmatic, dynamic, and interesting solar system bodies, demanding further study to elucidate its mysteries. Unfortunately its proximity to Jupiter places it in a high radiation zone, resulting in damage to optics and electronics, and reducing both the lifetime and the likelihood of a dedicated mission to Io. Fortunately the other Jovian moons are also high on

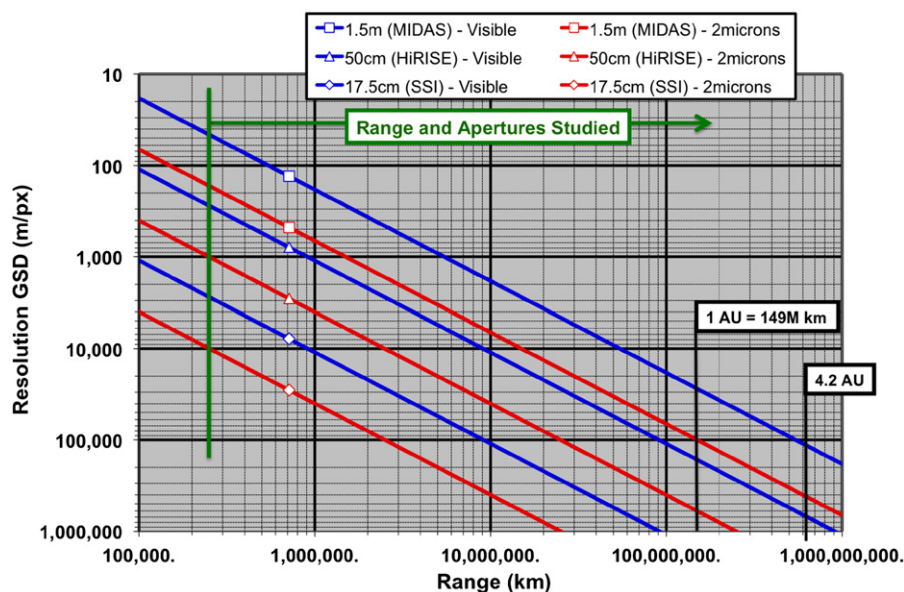


Fig. 9. Relative resolutions, in GSD, as a function of aperture size and distance.

the priority list for solar system science. In this paper, we show that a Europa or Ganymede orbiter would be capable of studying Io's surface in depth given sufficient resolution and wavelength coverage to enable a significant advance in our understanding of this moon.

Using high resolution images of a terrestrial volcano we have approximated the science return for long-range remote sensing of Io by both a 0.5 and 1.5 m telescope flown to the Jovian system. Several alternatives are currently available for imagers and imaging spectrometers in these aperture sizes that are compatible with Flagship and New Frontiers class outer planets missions. Although our study focused on Io, the results can easily be extended to other objects in the Jovian system, such as Jupiter itself, rings, inner moons, and Callisto, and are equally applicable for system science objectives in other planetary systems.

Acknowledgments

This work was supported in part by the National Science Foundation Science and Technology Center for Adaptive Optics, managed by the University of California at Santa Cruz under cooperative agreement AST 98-76783, the National Science Foundation (grant AST 0406275), and the National Aeronautics and Space Administration HICIT Program (NASA Grant No. NNG05GA25G).

References

- Archinal, B.A., Davies, M.E., Colvin, T.R., Becker, T.L., Kirk, R.L., Gitlin, A.R., 2001. An Improved RAND-USGS Control Network and Size Determination for Io, Lunar and Planetary Institute Science Conference Abstracts, 32, March 1, 2001.
- Belton, M.J.S., Klaasen, K.P., Clary, M.C., Anderson, J.L., Anger, C.D., Carr, M.H., Chapman, C.R., Davies, M.E., Greeley, R., Anderson, D., Bolef, L.K., Townsend, T.E., Greenberg, R., Head, J.W., Neukum, G., Pilcher, C.B., Veverka, J., Gierasch, P.J., Fanale, F.P., Ingersoll, A.P., Masursky, H., Morrison, D., Pollack, J.B., 1992. The Galileo solid-state imaging experiment. *Space Science Reviews (Historical Archive)* 60 (1–4), 413–455.
- Bergstrom, J.W., Delamere, A.W., McEwen, A.S., 2004. MRO high resolution imaging science experiment (HiRISE): instrument calibration and operating constraints. IAC-04-Q.3.b.02, 7.
- Blaney, D.L., Johnson, T.V., Matson, D.L., Veeder, G.J., 1995. Volcanic eruptions on Io: heat flow, resurfacing, and lava composition. *Icarus* 113, 220–225.
- de Pater, I., Marchis, F., Macintosh, B.A., Roe, H.G., Le Mignant, D., Graham, J.R., Davies, A.G., 2004. Keck AO observations of Io in and out of eclipse. *Icarus* 169, 250–263.
- de Pater, I., Laver, C., Marchis, F., Roe, H.G., Macintosh, B.A., 2007. Spatially resolved observations of the forbidden $SO\ a^1\Delta - X^3\Sigma^-$ rovibronic transition on Io during an eclipse and a volcanic eruption at Ra Patera. *Icarus* 191, 172–182.
- de Pater, I., Roe, H., Graham, J.R., Strobel, D.F., Bernath, P., 2002. Note: detection of the forbidden $SO\ a^1\Delta - X^3\Sigma^-$ rovibronic transition on Io at 1.7 μm . *Icarus* 156, 230–296.
- Dial, G., Bowen, H., Gerlach, F., Grodecki, J., Oleszczuk, R., 2003. IKONOS satellite, imagery, and products. *Remote Sensing of Environment* 88 (1–2), 23–36. doi:10.1016/j.rse.2003.08.014.
- Douté, S., Lopes, R., Kamp, L.W., Carlson, R., Schmitt, B., 2004. Geology and activity around volcanoes on Io from the analysis of NIMS spectral images. *Icarus* 169, 175–196.
- Douté, S., Schmitt, B., Lopes-Gautier, R., Carlson, R., Soderblom, L., Shirley, J., The Galileo NIMS Team, T. G. N. T., 2001. Mapping SO_2 frost on Io by the modeling of NIMS hyperspectral images. *Icarus* 149, 107–132.
- Geissler, P., McEwen, A., Phillips, C., Keszthelyi, L., Spencer, J., 2004. Surface changes on Io during the Galileo mission. *Icarus* 169, 29–64.
- Johnson, T.V., Veeder, G.J., Matson, D.L., Brown, R.H., Nelson, R.M., 1988. Io evidence for silicate volcanism in 1986. *Science* 242, 1280–1283.
- Kendrick, R.L., Smith, E.H., Duncan, A.L., 2003. Imaging Fourier transform spectrometry with a Fizeau interferometer. In: Shao, M. (ed.), *Proceedings of the SPIE*, vol. 4852. Interferometry in Space, February 2003, pp. 657–662.
- Kendrick, R.L., Aubrun, J.-N., Bell, R., Benson, R., Benson, L., Brace, D., Breakwell, J., Burriesci, L., Byler, E., Camp, J., Cross, G., Cuneo, P., Dean, P., Digumerthi, R., Duncan, A., Farley, J., Green, A., Hamilton, H.H., Herman, B., Lauritis, K., de Leon, E., Lorell, K., Martin, R., Matosian, K., Muench, T., Ni, M., Palmer, A., Roseman, D., Russell, S., Schweiger, P., Sigler, R., Smith, J., Stone, R., Stubbs, D., Swietek, G., Thatcher, J., Tischhauser, C., Wong, H., Zarifis, V., Gleichman, K., Paxman, R., 2006. Wide-field Fizeau imaging telescope: experimental results. *Applied Optics* 45, 4235–4240 2006.
- Laver, C., de Pater, I., 2008. Spatially resolved SO_2 ice on Io, observed in the near IR. *Icarus* 195, 752–757.
- Lucke, R., 2001. Fundamentals of wide-field sparse-aperture imaging. *Proceedings of the IEEE Aerospace Conference* 3, 1401–1419.
- Macintosh, B., Gavel, D., Gibbard, S.G., Max, C.E., de Pater, I., Ghez, A., Spencer, J., 2003. Speckle imaging of volcanic hot spots on Io with the Keck telescope. *Icarus* 165, 137–143.
- Marchis, F., de Pater, I., Davies, A.G., Roe, H.G., Fusco, T., Le Mignant, D., Descamps, P., Macintosh, B., Prange, R., 2002. High-resolution Keck adaptive optics imaging of violent volcanic activity on Io. *Icarus* 160, 124–131.
- Marchis, F., Descamps, P., Hestroffer, D., Berthier, J., Vachier, F., Boccaletti, A., de Pater, I., Gavel, D., 2003. A three-dimensional solution for the orbit of the asteroidal satellite of 22 Kalliope. *Icarus* 165, 112–120.
- McEwen, A.S., 1988. Global color and albedo variations on Io. *Icarus* 73, 385–426.
- McEwen, A.S., Belton, M.J.S., Breneman, H.H., Fagents, S.A., Geissler, P., Greeley, R., Head, J.W., Hoppa, G., Jaeger, W.L., Johnson, T.V., Keszthelyi, L., Klaasen, K.P., Lopes-Gautier, R., Magee, K.P., Milazzo, M.P., Moore, J.M., Pappalardo, R.T., Phillips, C.B., Radebaugh, J., Schubert, G., Schuster, P., Simonelli, D.P., Sullivan, R., Thomas, P.C., Turtle, E.P., Williams, D.A., 2000. Galileo at Io:

- Results from High-Resolution Imaging. *Science*, 288 (5469), 1193–1198. doi:10.1126/science.288.5469.1193.
- McEwen, A.S., Simonelli, D.P., Senske, D.R., Klaasen, K.P., Keszthelyi, L., Johnson, T.V., Geissler, P.E., Carr, M.H., Belton, M.J.S., 1997. High-temperature hot spots on Io as seen by the Galileo solid state imaging (SSI) experiment. *Geophysical Research Letters* 24, 2443–2446.
- McEwen, A.S., et al., 1998. High-temperature silicate volcanism on Jupiter's Moon Io. *Science* 281, 87–90.
- McEwen, A.S., Banks, M.E., Baugh, N., Becker, K., Boyd, A., Bergstrom, J.W., Beyer, R.A., Bortolini, E., Bridges, N.T., Byrne, S., Castaliar, B., Chuang, F.C., Crumpler, L.S., Daubar, I., Davatzes, A.K., Deardorff, D.G., Dejong, A., Alan Delamere, W., Dobra, E.N., Dundas, C.M., Eliason, E.M., Espinoza, Y., Fennema, A., Fishbaugh, K.E., Forrester, T., Geissler, P.E., Grant, J.A., Griffes, J.L., Grotzinger, J.P., Gulick, V.C., Hansen, C.J., Herkenhoff, K.E., Heyd, R., Jaeger, W.L., Jones, D., Kanefsky, B., Keszthelyi, L., King, R., Kirk, R.L., Kolb, K.J., Lasco, J., Lefort, A., Leis, R., Lewis, K.W., Martinez-Alonso, S., Mattson, S., McArthur, G., Mellon, M.T., Metz, J.M., Milazzo, M.P., Milliken, R.E., Motazedian, T., Okubo, C.H., Ortiz, A., Philippoff, A.J., Plassmann, J., Polit, A., Russell, P.S., Schaller, C., Searls, M.L., Spriggs, T., Squyres, S.W., Tarr, S., Thomas, N., Thomson, B.J., Tornabene, L.L., Van Houten, C., Verba, C., Weitz, C.M., Wray, J.J., 2010. The high resolution imaging science experiment (HiRISE) during MRO's primary science phase (PSP). *Icarus* 205 (1), 2–37.
- McGrath, M.A., Belton, M.J.S., Spencer, J.R., Sartoretti, P., 2000. Spatially resolved spectroscopy of Io's pele plume and SO₂ atmosphere. *Icarus* 146, 476–493.
- Milazzo, M.P., Keszthelyi, L.P., Radebaugh, J., Davies, A.G., Turtle, E.P., Geissler, P., Klaasen, K.P., Rathbun, J.A., McEwen, A.S., 2005. Volcanic activity at Tvashtar Catena, Io. *Icarus* 179, 235–251.
- Minnaert, M., 1941. The reciprocity principle in lunar photometry. *Astrophysics Journal* 93, 403–410.
- Pitman, J.T., A. Duncan, D. Stubbs, R.D., Sigler, R.L., Kendrick, E.H., Smith, J.E., Mason, G., Delory, J.H., Lipps, M., Manga, J.R., Graham, I., de Pater, S., Rieboldt, E., Bierhaus, J.B., Dalton, J.R., Fienup, J.W., Yu, 2004a. Remote sensing space science enabled by the multiple instrument distributed aperture sensor (MIDAS) concept. in: Hoover, R.B., Levin, G.V., Rozanov, A.Y. (eds.), *Proceedings of SPIE*, vol. 5555. Instruments, Methods, and Missions for Astrobiology VIII, November 2004, pp. 301–310.
- Pitman, J.T., Duncan, A., Stubbs, D., Sigler, R.D., Kendrick, R.L., Smith, E.H., Mason, J.E., Delory, G., Lipps, J.H., Manga, M., Graham, J.R., de Pater, I., Reiboldt, S., Marcus, P., Bierhaus, E., Dalton, J.B., Fienup, J.R., Yu, J.W., 2004b. Multiple instrument distributed aperture sensor (MIDAS) for planetary remote sensing. In: Nardell, C.A., Lucey, P.G., Yee, J., Garvin, J.B. (eds.), *Proceedings of SPIE*, vol. 5660. Instruments, Science and Methods for Geospace and Planetary Remote Sensing, December 2004, pp. 168–180.
- Rathbun, J.A., Spencer, J.R., Davies, A.G., Howell, R.R., Wilson, L., 2002. Loki, Io: a periodic volcano. *Geophysical Research Letters* 29, 81–84.
- Retherford, K.D., Spencer, J.R., Stern, S.A., Saur, J., Strobel, D.F., Steffl, A.J., Gladstone, G.R., Weaver, H.A., Cheng, A.F., Parker, J.W., Slater, D.C., Versteeg, M.H., Davis, M.W., Bagenal, F., Throop, H.B., Lopes, R.M.C., Reuter, D.C., Lunsford, A., Conard, S.J., Young, L.A., Moore, J.M., 2007. Io's atmospheric response to eclipse: UV aurora observations. *Science* 318, 237.
- Ryan, R., Baldrige, B., Schowengerdt, R.A., Choi, T., Helder, D.L., Blonski, S., 2003. IKONOS spatial resolution and image interpretability characterization. *Remote Sensing of Environment* 88 (1–2), 37–52. doi:10.1016/j.rse.2003.07.006.
- Smith, E.H., de Leon, E., Dean, P., Deloumi, J., Duncan, A., Hoskins, W., Kendrick, R., Mason, J., Page, J., Phenix, A., Pitman, J., Pope, C., Privari, B., Ratto, D., Romero, E., Shu, K., Sigler, R., Stubbs, D., Tapos, F., Yee, A., 2005. Multiple instrument distributed aperture sensor (MIDAS) testbed. In: Butler, X.J.J. (ed.), *Proceedings of SPIE*, vol. 5882. Earth Observing Systems, August 2005, Paper 5882-1F.
- Spencer, J.R., Lellouch, E., Richter, M.J., López-Valverde, M.A., Jessup, K.L., Great-house, T.K., Flaud, J.M., 2005. Mid-infrared detection of large longitudinal asymmetries in Io's SO₂ atmosphere. *Icarus* 176, 283–304.
- Spencer, J.R., Stern, S.A., Cheng, A.F., Weaver, H.A., Reuter, D.C., Retherford, K., Lunsford, A., Moore, J.M., Abramov, O., Lopes, R.M.C., Perry, J.E., Kamp, L., Showalter, M., Jessup, K.L., Marchis, F., Schenk, P.M., Dumas, C., 2007. Io volcanism seen by new horizons: a major eruption of the tvashtar volcano. *Science* 318, 240–243.
- Stubbs, D.M., Duncan, A.L., Pitman, J.T., Sigler, R.D., Kendrick, R.L., Chilese, J.F., Smith, E.H., 2004. Multiple instrument distributed aperture sensor (MIDAS) science payload concept. in: Mather, J.C. (ed.), *Proceedings of SPIE*, vol. 5487. Optical, Infrared, and Millimeter Space Telescopes, October 2004, pp. 1444–1452.
- Turtle, E.P., Keszthelyi, L.P., McEwen, A.S., Radebaugh, J., Milazzo, M., Simonelli, D.P., Geissler, P., Williams, D.A., Perry, J., Jaeger, W.L., Klaasen, K.P., Breneman, H.H., Denk, T., Phillips, C.B., 2004. The final Galileo SSI observations of Io: orbits G28–I33. *Icarus* 169, 3–28.
- Williams, D.A., Wilson, A.H., Greeley, R., 2000. A komatiite analog to potential ultramafic materials on Io. *Journal of Geophysical Research* 105, 1671–1684.
- Williams, D.A., et al., 2009. Future Io exploration for 2013–2022 and beyond, part 1: justification and science objectives. *Planetary Decadal Study Community White Paper Solar System Exploration Survey, 2013–2022*.
- Zariffs, V., Bell, R.M. Jr., Benson, L.R., Cuneo, P.J., Duncan, A.L., Herman, B.J., Holmes, B., Sigler, R.D., Stone, R.E., Stubbs, D.M., 1999. The multi aperture imaging array. In: Unwin and Stachnik (eds.), *ASP Conference Series* 194, 1999, p. 278.